



Article

# The Preparation of N-Doped Titanium Dioxide Films and Their Degradation of Organic Pollutants

Yanyan Dou <sup>1</sup>, Yixuan Chang <sup>1</sup>, Xuejun Duan <sup>1,\*</sup>, Leilei Fan <sup>2</sup>, Bo Yang <sup>3,\*</sup> and Jingjing Lv <sup>1</sup>

<sup>1</sup> School of Energy and Environment, Zhongyuan University of Technology, Zhengzhou 450007, China

<sup>2</sup> Department of Resources and Environment, Zunyi Normal College, Zunyi 563006, China

<sup>3</sup> People's Government of Donganggezhuang Town, Luanzhou City, Tangshan 063000, China

\* Correspondence: 5529@zut.edu.cn (X.D.); 2021108299@zut.edu.cn (B.Y.)

**Abstract:** N-doped TiO<sub>2</sub> films supported by glass slides showed superior photocatalytic efficiency compared with naked TiO<sub>2</sub> powder due to them being easier to separate and especially being responsive to visible light. The films in this study were prepared via the sol–gel method using TBOT hydrolyzed in an ethanol solution and the nitrogen was provided by cabamide. The N-doped TiO<sub>2</sub> coatings were prepared via a dip-coating method on glass substrates (30 × 30 × 2 mm) and then annealed in air at 490 °C for 3 h. The samples were characterized using X-ray diffraction (XRD), scanning electron microscopy (SEM) and UV-vis. The doping rate of N ranged from 0.1 to 0.9 (molar ratio), which caused redshifts to a longer wavelength as seen in the UV-vis analysis. The photocatalytic activity was investigated in terms of the degradation of phenol under both UV light and visible light over 4 h. Under UV light, the degradation rate of phenol ranged from 86% to 94% for all the samples because of the sufficient photon energy from the UV light. Meanwhile, under visible light, a peak appeared at the N-doping rate of 0.5, which had a degrading efficiency that reached 79.2%, and the lowest degradation rate was 32.9%. The SEM, XRD and UV-vis experimental results were consistent with each other.



**Citation:** Dou, Y.; Chang, Y.; Duan, X.; Fan, L.; Yang, B.; Lv, J. The Preparation of N-Doped Titanium Dioxide Films and Their Degradation of Organic Pollutants. *Int. J. Environ. Res. Public Health* **2022**, *19*, 15721. <https://doi.org/10.3390/ijerph192315721>

Academic Editors: Xun Wang, Zhiyuan Wang and Xin Zhao

Received: 20 October 2022

Accepted: 23 November 2022

Published: 25 November 2022

**Publisher's Note:** MDPI stays neutral with regard to jurisdictional claims in published maps and institutional affiliations.



**Copyright:** © 2022 by the authors. Licensee MDPI, Basel, Switzerland. This article is an open access article distributed under the terms and conditions of the Creative Commons Attribution (CC BY) license (<https://creativecommons.org/licenses/by/4.0/>).

**Keywords:** photocatalysis; N-doped films; visible light; titanium dioxide

## 1. Introduction

In recent years, substances that cause water pollution are mainly refractory pollutants in industrial and agricultural wastewater and domestic sewage, such as volatile halogenated hydrocarbons, phenols, nitrobenzene and polycyclic aromatic hydrocarbons. Much effort has been devoted to the photocatalysis field in water treatment to efficiently remove nonbiodegradable compounds and avoid secondary pollution. The photocatalytic reaction transfers an electron from a valance band electron to an empty conduction band by absorbing photon energy equal to or more than the semiconductor band gap. The resulting electron–hole pairs contribute to the degradation reaction of the pollutant. Phenolic compounds are highly toxic and carcinogenic; they are present in wastewater, mainly in effluents from the production of pharmaceuticals, plastics, pesticides, oil and petrochemicals. Phenol was used as a model form of pollution since its molecular structure contains a benzene ring, making it quite stable and difficult to be biodegraded.

Common semiconductor photocatalysts include TiO<sub>2</sub>, WO<sub>3</sub>, ZnO and NiO. In order to improve the photocatalytic degradation activity, many technologies were proposed, such as metal or nonmetal doping, the development of microspheres and coupling semiconductors together. A pure TiO<sub>2</sub> photocatalyst often has some shortcomings, such as easy recombination of photogenerated electrons and holes, low catalytic efficiency and only responds to UV light, which limits its practical application. To solve these problems, current research focuses on metal/nonmetallic element doping, precious metal deposition and the construction of composite photocatalysts. TiO<sub>2</sub> of ultrafine nanoparticle size is considered to be

the most useful photocatalyst for its excellent properties, such as high-light-conversion efficiency, chemical stability, nontoxic nature and low cost [1–13].

The band gap energy of  $\text{TiO}_2$  is 3.2 eV (for anatase) and 3.0 eV (for rutile), and the maximum absorption wavelength of  $\text{TiO}_2$  is 387.5 nm (anatase); that is to say,  $\text{TiO}_2$  can only assimilate UV light rather than generate electrons ( $e^-$ ) and holes ( $h^+$ ), which can subsequently induce redox reactions for the degradation of nonbiodegradable organics in water [14]. Under the irradiation of UV light, electrons are promoted from the valence band to the conduction band of the semiconductor, creating electron–hole pairs, which can cause highly oxidizing hydroxyl and highly reduced superoxide radicals [15]. While the energy of UV light only takes 4–5% of the solar energy, how to enlarge the maximum absorption wavelength of  $\text{TiO}_2$  for visible light and cause  $\text{TiO}_2$  to absorb more visible light has become a research hotspot in recent years [16]. Ion doping, semiconductor complexes and surface photosensitized methods were employed to cause  $\text{TiO}_2$  to be responsive to visible light. Nonmetallic ion doping is one of the widely studied ways of inducing new electronic bands and optical transitions, which involves the inclusion or substitution of a foreign atom, such as nitrogen, sulfur, fluorine or sulfur, that replaces the oxygen atom in the  $\text{TiO}_2$  crystal lattice [17–19]. Doping  $\text{TiO}_2$  with nitrogen can create a redshift in the absorption wavelength from UV to the visible range because of the formation of new states inside the  $\text{TiO}_2$  bandgap. This shift could enable photocatalytic reactions to produce a high degradation rate under sunlight illumination [20–23].

Different nano- $\text{TiO}_2$  photocatalytic systems in suspension were studied, such as nanoparticles, nanobelts and nanotubes, where  $\text{TiO}_2$  has a larger specific surface area and high absorption of light, and all show increased photocatalytic activity when excited under visible light toward the degradation of different chemical species [24–26]. However, difficulties in separation and recycling lead to the smaller possibility of industrial application. Furthermore, the dosage of  $\text{TiO}_2$  is difficult to control, where too little will lead to low photocatalytic efficiency and too much will cause light scattering that influences the absorption of light. Thus, much effort was expended to immobilize photocatalysts in the form of thin films on a stable support to avoid the problems associated with disposing photocatalyst suspensions [27]. Different contents of doped nitrogen have different impacts on the photocatalytic efficiency, for disparities in the replaced oxygen atom can lead to variations in the photocatalyst activity. Frequently used nitrogen sources include urea, triethylamine, ammonia and ethylmethanamine [25].

N-doped  $\text{TiO}_2$  thin films can effectively solve the previous problems by enlarging the maximum absorption wavelength and realizing immobilization together. Nitrogen is doped into  $\text{TiO}_2$  using the sol–gel method, which is easy to operate and the reaction condition is mild. The formation of catalyst needs to go through the procedure of dipping, pulling out, drying, annealing, and chilling [28].

The purpose of this research was to prepare nitrogen-doped  $\text{TiO}_2$  thin films on sheet substrates of different nitrogenous amounts using the sol–gel method. The advantages of this method are that  $\text{TiO}_2$  can be stimulated with visible light, it solves the traditional issue of photocatalytic technology being difficult to control, problems such as high cost and effective components being easily lost are solved, and it greatly improves the possibility of a large-scale practical application in wastewater treatment engineering. We compared the degradation properties of these samples, investigated degradation results and their characterization consequences, analyzed the influence of the amount of nitrogen, and addressed the relationship between the concentration of zymolyte and the reaction time.

## 2. Materials and Methods

### 2.1. Materials and Reagent

Tetrabutyltitanate (CP, 98%), acetylacetone (AR, 98.0%), polyethylene glycol, acetone (AR, 99.5%) and hydrofluoric acid were provided by GuangFu Fine Chemical Research Institution in Tianjin. Anhydrous ethanol (AR, 99.7%) and carbamide (AR, 99.5%) were made by ShuangShuang Chemical Co., Ltd., in YanTai, China. Deionized water was created

in our lab. The glass substrates used were common commercial glass sheets cut to the needed size.

### 2.2. Preparation of N-Doped TiO<sub>2</sub> Films

The dip-coating method was utilized to immobilize the films. Precursor solutions for N-doped TiO<sub>2</sub> coatings were prepared with tetrabutyltitanate, anhydrous ethanol, acetylacetone, carbamide, deionized water and polyethylene glycol (1 wt%). Tetrabutyltitanate (20 mL), anhydrous ethanol (80 mL) and acetylacetone (3 mL) were mixed using magnetic stirring for 20 min, followed by a certain quantity of carbamide added into the solution as the donor of nitrogen (the molar ratios of N/Ti used were 0.1, 0.3, 0.5, 0.7 and 0.9). Deionized water (15 mL) was dropwise added at the speed of one drop per second and left to stir for one hour; then, the procedure was finished after the addition of polyethylene glycol (1 mL) to avoid fracturing of the films [28]. Undoped TiO<sub>2</sub> sol with the same reagents and procedures was also prepared to compare the photocatalytic activity with N-doped coatings. The sol was aged for 24 h at 35 °C and then used to make the coatings.

Commercial glass substrates (30 mm × 30 mm × 2 mm) cleaned with acetone (10 wt%) and eroded with hydrofluoric acid (10 wt%) for 3 h were used as the support of the N-doped TiO<sub>2</sub> films. The substrates were maintained in the aged sol for 10 min and then pulled out at the rate of 2 cm/s using a dip coater (CZ-4200, Qingdao Zhongrui Intelligent Instrument Co., LTD, Qingdao, China). After the films dried out, the previous process was repeated another three times; the product was then calcined for 3 h at 490 °C. The films were finally even and tight on the glass sheet. The coatings obtained were named TN0, TN1, TN3, TN5, TN7 and TN9 according to the amount of doped nitrogen.

### 2.3. Characterization

After the deposition of the TiO<sub>2</sub> films onto glass substrates, all of the remaining sol was dried at 80 °C for 20 h in order to obtain dried gels, which were then calcined at 490 °C for 3 h to prepare the powders with the same crystal phase as the coatings. These powders were synthesized to analyze the phase compositions of titania by means of X-ray diffraction (XRD) using a D/Max-2200 Powder X-ray Diffractometer (XRD, D/Max-2200, Nippon Science Corporation, Tokyo, Japan) with Cu-K $\alpha$  radiation at 40 kV and 20 mA.

Scanning electron microscopy (SEM, SU8220, Hitachi hi-tech, Shanghai, China) was utilized in an air atmosphere to examine the morphological structure and grain size of the films coated on the glass. The vapor has its considerable impact on the dried sample before observation [29].

The UV-vis DRS measurements were recorded at room temperature for the dry-pressed disk samples using a UV-3600 UV-vis spectrophotometer (UV-3600 UV-vis, Shimadzu, Tokyo, Japan) equipped with an integrating sphere assembly within the range of 300–900 nm.

### 2.4. Measurement of Photocatalytic Activity

The experiments were carried out with the initial concentration of phenol equal to 10 mg/L at an ambient temperature (approximately 25 °C) and pressure. The photoreactor used an acrylic cuboid static opaque chamber (700 mm × 450 mm × 250 mm) equipped with a thermocouple to monitor the temperature during irradiation. The UV source was supplied by 6 ultraviolet tubes (20 W), which had a dominant wavelength of 254 nm. As for the visible light source, 6 ordinary fluorescent lamps (20 W) were employed to produce the longer wavelength light.

Each beaker contained 8 pieces of glass sheet supporting N-doped TiO<sub>2</sub> coatings of the same amount of doped nitrogen. The illuminant was about 15 cm from the bottom of the solution. The system was left in the dark for 30 min until reaching phenol adsorption equilibrium, and then a photocatalytic reaction was carried out under UV light or visible light. The samples were taken from the reactor for analysis every 30 min, where the samples were placed in a 2 cm quartz dish and the remaining concentrations were analyzed using 4-AAP

extraction spectrophotometry and UV-vis spectrophotometry (Photo Lab 6600 UV-Vis, WTW, Munich, Germany) at 510 nm. The photocatalysis reaction lasted for 4 h.

### 3. Results and Discussion

#### 3.1. XRD Analysis

Figure 1 shows the XRD patterns of the six powdery samples. For all samples, it can be observed that where the  $2\theta$  was  $25.4^\circ$  (101), the diffraction peak was especially distinct, and at  $2\theta = 30.7^\circ$  (121), the relative intensity is quite small, which means that the anatase phase was dominant and the rutile phase was hardly existing. In addition, other characteristic peaks ( $2\theta = 25.34^\circ$ ,  $48.11^\circ$  and  $44.49^\circ$ ) were all accordant with JPDS-21-1272 [30] (anatase standard card). It can be confirmed that N-doped  $\text{TiO}_2$  mainly existed in the form of anatase. With the increase in the N doping amount, the sample pattern almost did not change, indicating that N doping had little effect on the crystal structure. The difference being all samples on the 101 crystal plane may have been caused by the grinding of the samples with different N contents.

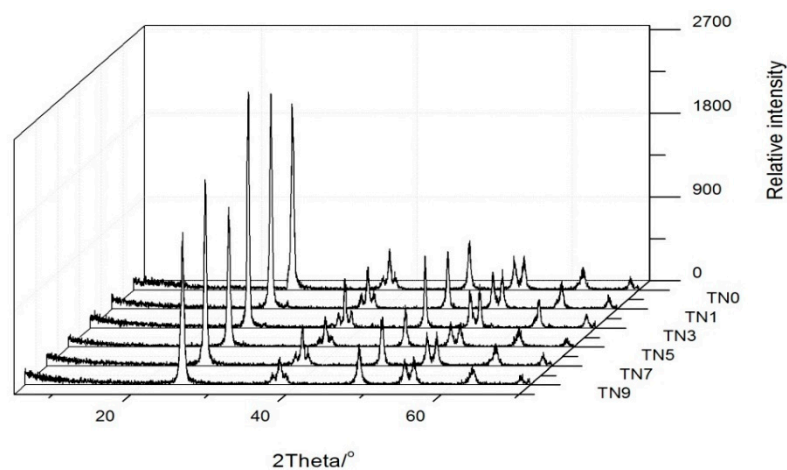
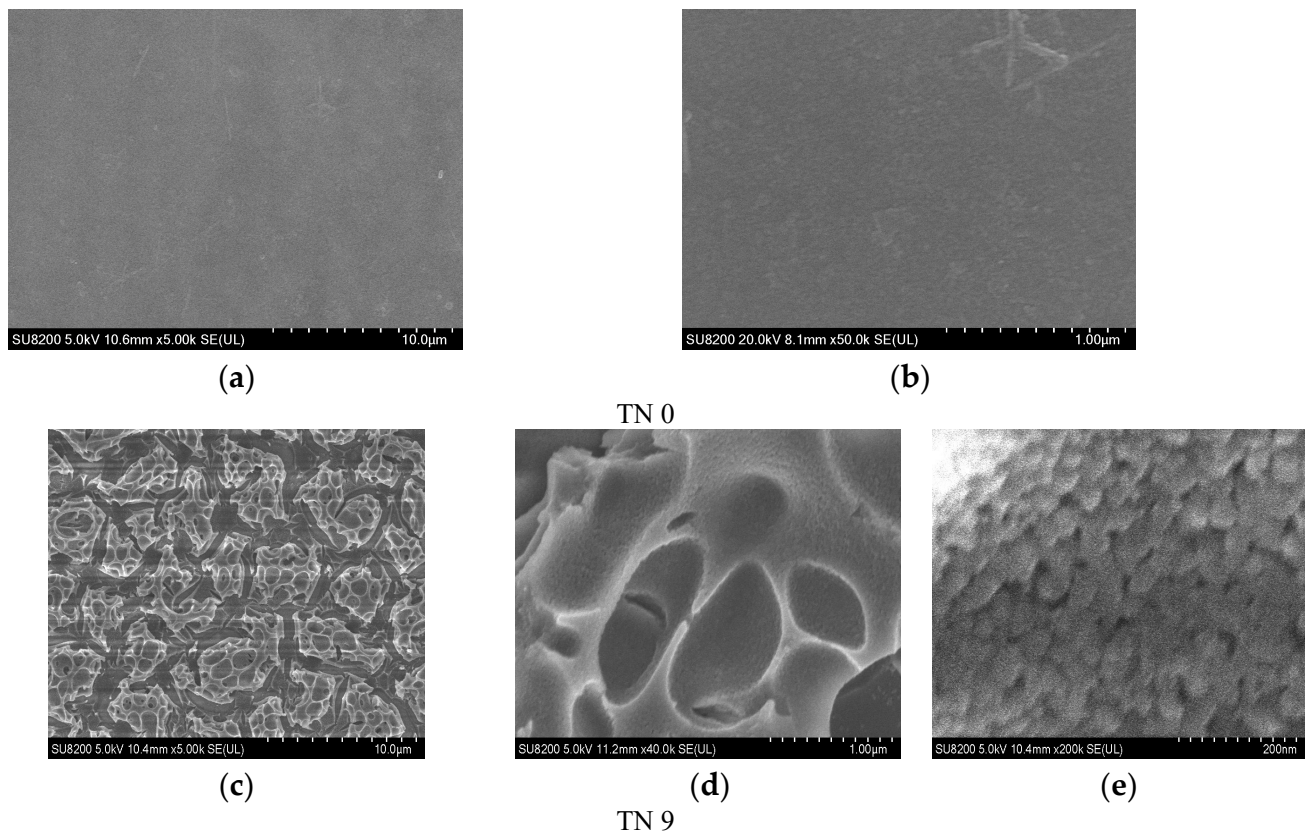


Figure 1. XRD patterns of TN0, TN1, TN3, TN5, TN7 and TN9.

#### 3.2. SEM Analysis

Figure 2 shows the SEM photographs of a clean glass substrate and N-doped  $\text{TiO}_2$  films. The glass substrate after being washed with acetone and eroded with hydrofluoric acid was quite clean and had an even roughness with a great transmission of light. A rough surface can increase the capacity of the load [27]. The microstructures of the six samples had no obvious differences, which indicated that the quantity of carbamide had little impact on the surface of the coatings. Figure 2d, e demonstrate that the films made using the sol-gel method were porous and the granules dispersed uniformly with particle sizes ranging from 30 nm to 80 nm.



**Figure 2.** SEM photographs of a clean glass substrate (a,b) (TN0) and SEM photographs of sample TN9 (c–e).

### 3.3. UV-Vis DRS Analysis

UV-vis DRS results are shown in Figure 3. The maximum absorption wavelength of TN0 was about 380 nm, indicating the main components of samples were naked titanium dioxide with little impurities. Different amounts of N-doping replaced oxygen atoms in the  $\text{TiO}_2$  crystal lattice with nitrogen atoms to different degrees, which was also the reason for different degrees of redshift when compared with the maximum absorption wavelength of TN0. It is worth noting that the nitrogen doping amount did not follow a “the more, the better” pattern within a certain range since the maximal redshift occurred for TN5, not TN9. Different amounts of N-doping can reduce the bandwidth of  $\text{TiO}_2$ , enhance the transfer of electrons from the valence band to the conduction band and improve the photocatalytic rate. However, when the amount of N-doping is too much, the nitrogen atom will become the center of electron recombination and accelerate the recombination rate of electrons and holes, thus affecting the photocatalytic rate [31,32].

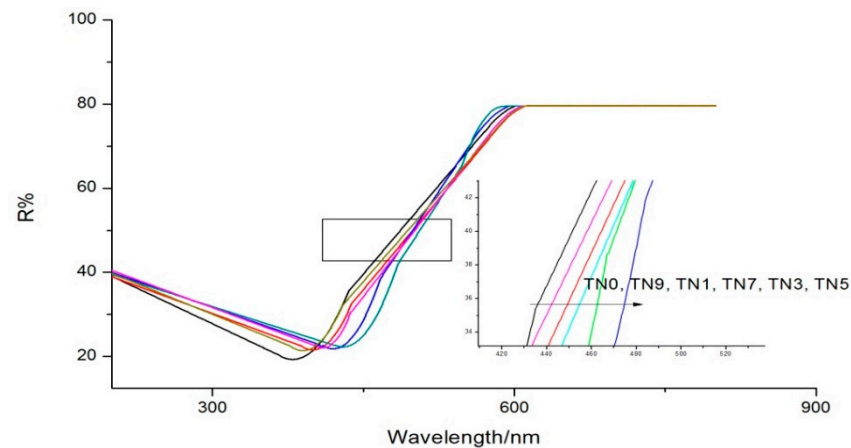


**Figure 3.** UV-vis DRS of TN0, TN1, TN3, TN5, TN7 and TN9.

### 3.4. Photocatalytic Activity under UV and Visible Light Irradiation

#### 3.4.1. Photocatalytic Activity under UV Light Irradiation

With regard to absorption, the dark test showed that the variation of phenol concentration caused by absorption was lower than 3%, which meant that the absorption had little influence on the degradation ratio of the photocatalytic procedure.

The variation of each sample over time is shown in Figure 4. The phenol concentration at 0 min was measured just after absorption. It can be observed that the rank of the six samples regarding photocatalytic activity was TN5 > TN3 > TN7 > TN1 > TN9 > TN0, i.e., TN5 had the highest degradation over the others during the same period. The degradation ratios were 93.77%, 91.32%, 90.82%, 88.89%, 85.73% and 80.10%, respectively. The maximum absorption wavelength of the five N-doped samples were all redshifted to visible light to different degrees, while the photocatalytic activities of the five samples were also enhanced, which should have been caused by the doping nitrogen leading to the energy structure of titanium dioxide changed; that is to say, the optical energy band gap of TiO<sub>2</sub> diminished. A reduction in the optical energy band gap will enhance the transfer of electrons from the valence band to the conduction band under visible light, which may have been the reason for the better relative performance of the N-doped TiO<sub>2</sub> [33]. The kinetics of phenol removal followed the Langmuir–Hinshelwood kinetic equation [34]:

$$R = d_c/d_t = kK_c/(1 + K_c) \quad (1)$$

where  $R$  represents the reaction rate,  $c$  is the concentration of the substrate at the time,  $k$  is the reaction rate constant and  $K_c$  is the adsorption constant. When the concentration was very low,  $K_c \ll 1$ ; therefore, the relevant equation turned out to be

$$\ln(c_0/c) = k_t + b \quad (2)$$

where  $c_0$  is the initial concentration,  $t$  is the reaction time and  $k_t$  is the apparent reaction rate constant. Figure 5 shows the kinetics of the six samples. The apparent reaction rate constants ranged from 0.00614 to 0.01048.

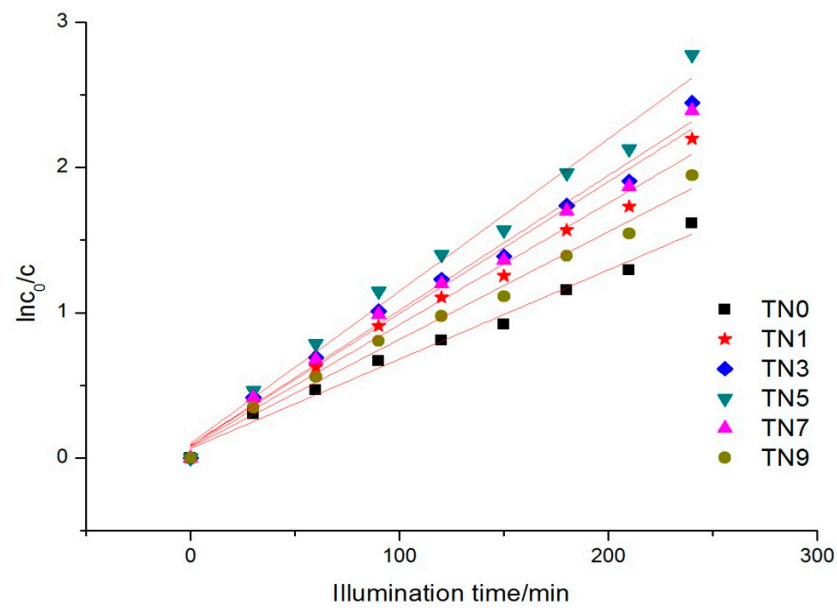


Figure 4. Phenol concentration trend under UV light.

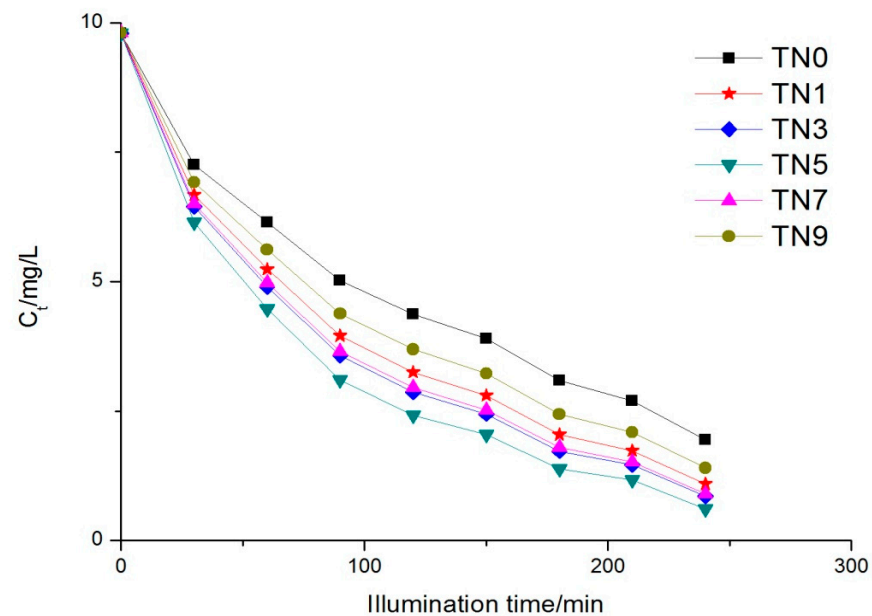
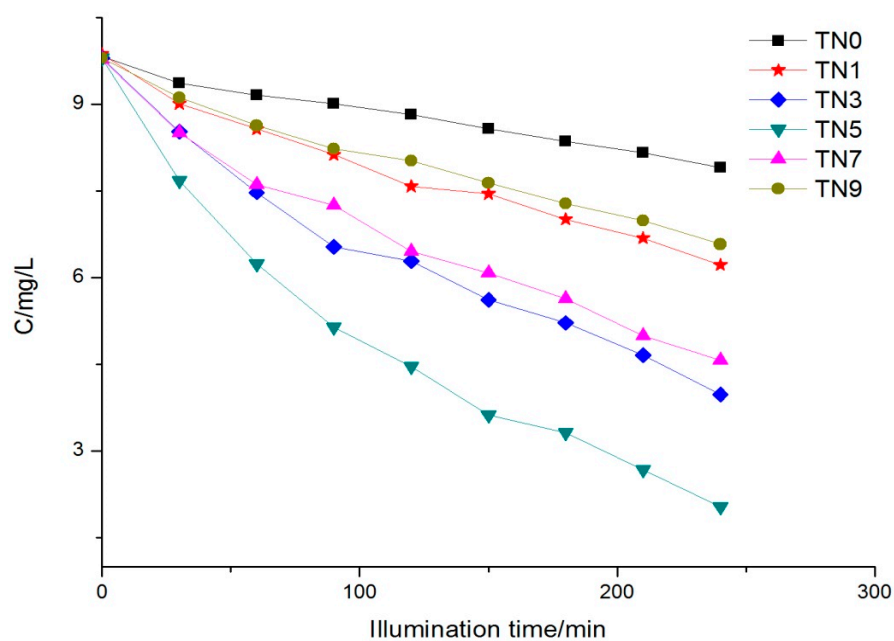


Figure 5. Reaction kinetics trend under UV light.

#### 3.4.2. Photocatalytic Activity under Visible Light Irradiation

The absorption under visible light in the dark period made little difference compared with UV light, while the variation in phenol concentration during illumination time made a significant difference.

It can be observed from Figure 6 that the degradation rates of the N-doped samples were obviously better than that of the naked  $\text{TiO}_2$  (TN0). TN5 still possessed the fastest degradation rate, followed by TN3, TN7, TN1 and TN9; that is to say, the best degradation efficiency appeared at the point where the molar ratio of N/Ti was 0.5, rather than the more nitrogen doping, the higher the degradation rate. The degradation results were also coincident with the UV-vis DRS results, where TN5 had the greatest redshift.



**Figure 6.** Phenol concentration trend under visible light.

The kinetics of phenol removal under visible light also followed the Langmuir–Hinshelwood kinetic equation (the kinetic Equation (1) in 3.4.1), as Figure 7 shows. The apparent reaction rate constants ranged from 0.00156 to 0.04893.

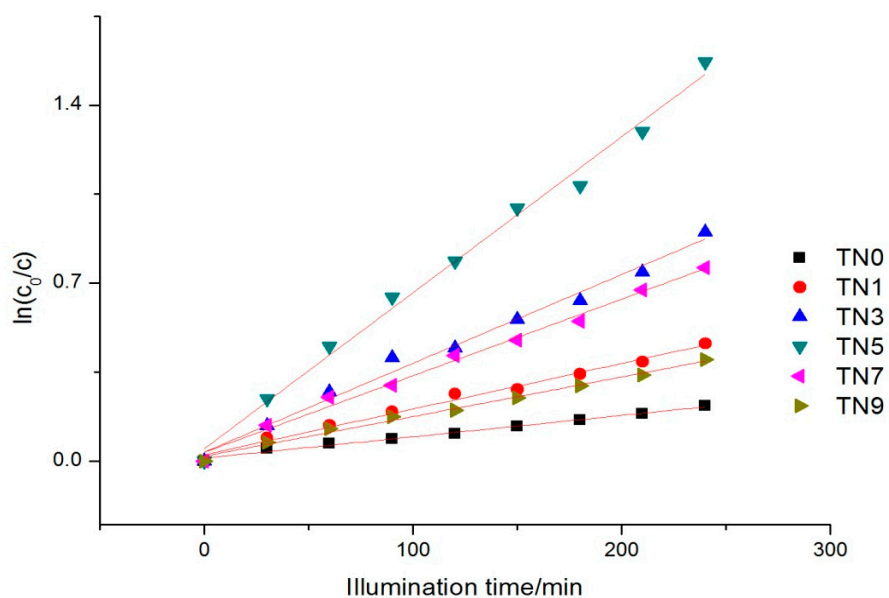


**Figure 7.** Reaction kinetics trend under visible light.

#### 4. Conclusions

N-doped TiO<sub>2</sub> thin films were successfully immobilized on commercial glass substrates via the sol–gel method starting from tetrabutyltitanate dissolving in anhydrous ethanol as a precursor. The formulation of sol and an annealing temperature of 490 °C were optimal, as seen by the highly uniform lattice structure that was mainly constituted of anatase and the TiO<sub>2</sub> granules being evenly distributed with ultrafine nano-particle sizes ranging from 30 to 80 nm. The surface morphology of the coating was basically unaffected by different nitrogen contents. Under the same experimental conditions, the degradation efficiency of phenol in the experimental group under visible light irradiation reached about 90% of that

under UV light, indicating that N-doping caused the optical energy band gap of TiO<sub>2</sub> to diminish; therefore, the maximum absorption wavelength had obvious redshifts, leading to the doped films having more efficient photocatalytic activity, both under UV light and visible light. The optimal photocatalytic efficiency was realized at an N-doping ratio of 0.5, rather than the more dopant, the better the photocatalytic efficiency since an excess N-doping ratio leads to an increased recombination ratio of electrons and holes, which reduces the photon utilization factor. The pollution absorption ability of the TiO<sub>2</sub> and glass sheet was quite feeble; thus, the kinetics of degradation followed the Langmuir–Hinshelwood kinetic equation, which describes first-order reaction kinetics.

**Author Contributions:** Y.D. and L.F. contributed substantially to the design of the study, the analyses, the writing of the manuscript and the original draft preparation. X.D. and J.L. contributed to the project administration, the funding acquisition and verifying the experimental data. Y.C. and B.Y. took responsibility for performing the experiments and validation and made the figures, replied to comments and corrected the draft. All authors have read and agreed to the published version of the manuscript.

**Funding:** This work was supported by the Project of Guizhou Education, Science and Technology Project of Guizhou Province ([2016]1163), the Project of Guizhou Education Department([2016]047), the Training Program for Young Backbone Teachers in Colleges and Universities of Henan Province, (no. 2019GGJS140), the Zunyi Science and Technology Planning Project (no. ZSKH(2021)199), the 2021 Rural Revitalization Project of Zunyi Normal University (Special Scientific Research Fund of Guizhou Provincial Department of Education) (QJHKY [2021]017-9), the Zunyi Normal University Serving Local Industrial Revolution project (N0.ZSCXY [2021]04) and the “2021 academic new seedling cultivation and innovation exploration project” of Zunyi Normal University (no. ZSXM [2021]1-10).

**Institutional Review Board Statement:** Not applicable.

**Informed Consent Statement:** Not applicable.

**Data Availability Statement:** Not applicable.

**Conflicts of Interest:** The authors declare no conflict of interest.

## References

1. Kudo, A.; Miseki, Y. Heterogeneous photocatalyst materials for water splitting. *Chem. Soc. Rev.* **2009**, *38*, 253–278. [[CrossRef](#)]
2. Kuwahara, Y.; Yamashita, H. Efficient photocatalytic degradation of organics diluted in water and air using TiO<sub>2</sub> designed with zeolites and mesoporous silica materials. *J. Mater. Chem.* **2011**, *21*, 2407–2416. [[CrossRef](#)]
3. Liu, D.; Cui, W.; Lin, J.; Xue, Y.; Huang, Y.; Li, J.; Zhang, J.; Liu, Z.; Tang, C. A novel TiO<sub>2</sub>—xNx/BN composite photocatalyst: Synthesis, characterization and enhanced photocatalytic activity for Rhodamine B degradation under visible light. *Catal. Commun.* **2014**, *57*, 9–13. [[CrossRef](#)]
4. Khan, H.; Berk, D. Characterization and mechanistic study of Mo<sup>+6</sup> and V<sup>+5</sup> codoped TiO<sub>2</sub> as a photocatalyst. *J. Photochem. Photobiol. A Chem.* **2014**, *294*, 96–109. [[CrossRef](#)]
5. Yang, Y.; Zhang, T.; Le, L.; Ruan, X.; Fang, P.; Pan, C.; Xiong, R.; Shi, J.; Wei, J. Quick and Facile Preparation of Visible light-Driven TiO<sub>2</sub> Photocatalyst with High Absorption and Photocatalytic Activity. *Sci. Rep.* **2014**, *4*, 7045. [[CrossRef](#)]
6. Ljubas, D.; Franzreb, M.; Hansen, H.C.B.; Weidler, P.G. Magnetizing of nano-materials on example of Degussa’s P-25 TiO<sub>2</sub> photocatalyst: Synthesis of magnetic aggregates, characterization and possible use. *Sep. Purif. Technol.* **2014**, *136*, 274–285. [[CrossRef](#)]
7. Paul, T.; Machesky, M.L.; Strathmann, T.J. Correction to Surface Complexation of the Zwitterionic Fluoroquinolone Antibiotic Ofloxacin to Nano-Anatase TiO<sub>2</sub> Photocatalyst Surfaces. *Environ. Sci. Technol.* **2014**, *48*, 11736. [[CrossRef](#)]
8. Kamegawa, T.; Ishiguro, Y.; Kido, R.; Yamashita, H. Design of Composite Photocatalyst of TiO<sub>2</sub> and Y-Zeolite for Degradation of 2-Propanol in the Gas Phase under UV and Visible Light Irradiation. *Molecules* **2014**, *19*, 16477–16488. [[CrossRef](#)]
9. He, K.F.; Xu, E.N.; Liu, Y.; Chen, W.P. Hydrogenation of Nano-Structured TiO<sub>2</sub> Photocatalyst Through an Electrochemical Method. *J. Nanosci. Nanotechnol.* **2015**, *15*, 303–308. [[CrossRef](#)]
10. Naeimi, A.; Sharifi, A.; Montazerghaem, L.; Abhari, A.R.; Mahmoodi, Z.; Bakr, Z.H.; Soldatov, A.V.; Ali, G.A.M. Transition Metals Doped WO<sub>3</sub> Photocatalyst towards High Efficiency Decolourization of Azo Dye. *J. Mol. Struct.* **2022**, *1250*, 131800. [[CrossRef](#)]
11. Saad, A.M.; Abukhadra, M.R.; Ahmed, S.A.-K.; Elzanaty, A.M.; Mady, A.H.; Betiha, M.A.; Shim, J.J.; Rabie, A.M. Photocatalytic Degradation of Malachite Green Dye Using Chitosan Supported ZnO and Ce–ZnO Nano-Flowers under Visible Light. *J. Environ. Manag.* **2020**, *258*, 110043. [[CrossRef](#)]

12. Ethiraj, A.S.; Uttam, P.K.V.; Chong, K.F.; Ali, G.A.M. Photocatalytic Performance of a Novel Semiconductor Nanocatalyst: Copper Doped Nickel Oxide for Phenol Degradation. *Mater. Chem. Phys.* **2020**, *242*, 122520. [[CrossRef](#)]
13. Mandor, H.; Amin, N.K.; Abdelwahab, O.; El-Ashtoukhy, E.-S.Z. Preparation and Characterization of N-Doped ZnO and N-Doped TiO<sub>2</sub> Beads for Photocatalytic Degradation of Phenol and Ammonia. *Environ. Sci. Pollut. Res.* **2022**, *29*, 56845–56862. [[CrossRef](#)]
14. Fujishima, A.; Honda, K. Electrochemical Photolysis of Water at a Semiconductor Electrode. *Nature* **1972**, *238*, 37–38. [[CrossRef](#)] [[PubMed](#)]
15. Lui, G.; Liao, J.-Y.; Duan, A.; Zhang, Z.; Fowler, M.; Yu, A. Graphene-wrapped hierarchical TiO<sub>2</sub> nanoflower composites with enhanced photocatalytic performance. *J. Mater. Chem. A* **2013**, *1*, 12255–12262. [[CrossRef](#)]
16. Jaiswal, R.; Patel, N.; Dashora, A.; Fernandes, R.; Yadav, M.; Edla, R.; Varma, R.; Kothari, D.; Ahuja, B.; Miotello, A. Efficient Co-B-codoped TiO<sub>2</sub> photocatalyst for degradation of organic water pollutant under visible light. *Appl. Catal. B Environ.* **2016**, *183*, 242–253. [[CrossRef](#)]
17. Asahi, R.; Morikawa, T.; Ohwaki, T.; Aoki, K.; Taga, Y. Visible-Light Photocatalysis in Nitrogen-Doped Titanium Oxides. *Science* **2001**, *293*, 269–271. [[CrossRef](#)] [[PubMed](#)]
18. Yoshinaga, M.; Yamamoto, K.; Sato, N.; Aoki, K.; Morikawa, T.; Muramatsu, A. Remarkably enhanced photocatalytic activity by nickel nanoparticle deposition on sulfur-doped titanium dioxide thin film. *Appl. Catal. B Environ.* **2009**, *87*, 239–244. [[CrossRef](#)]
19. Ho, W.; Yu, J.C.; Lee, S. Synthesis of hierarchical nanoporous F-doped TiO<sub>2</sub> spheres with visible light photocatalytic activity. *Chem. Commun.* **2006**, *10*, 1115–1117. [[CrossRef](#)]
20. Gumy, D.; Rincon, A.G.; Hajdu, R.; Pulgarin, C. Solar photocatalysis for detoxification and disinfection of water: Different types of suspended and fixed TiO<sub>2</sub> catalysts study. *Sol. Energy* **2006**, *80*, 1376–1381. [[CrossRef](#)]
21. Robert, D.; Piscopo, A.; Heintz, O.; Weber, J.V. Photocatalytic detoxification with TiO<sub>2</sub> supported on glass-fibre by using artificial and natural light. *Catal. Today* **1999**, *54*, 291–296. [[CrossRef](#)]
22. Águia, C.; Ângelo, J.; Madeira, L.M.; Mendes, A. Photo-oxidation of NO using an exterior paint—Screening of various commercial titania in powder pressed and paint films. *J. Environ. Manag.* **2011**, *92*, 1724–1732. [[CrossRef](#)] [[PubMed](#)]
23. van Grieken, R.; Marugán, J.; Sordo, C.; Pablos, C. Comparison of the photocatalytic disinfection of E. coli suspensions in slurry, wall and fixed-bed reactors. *Catal. Today* **2009**, *144*, 48–54. [[CrossRef](#)]
24. Burda, C.; Lou, Y.; Chen, X.; Samia, A.C.S.; Stout, J.; Gole, J.L. Enhanced Nitrogen Doping in TiO<sub>2</sub> Nanoparticles. *Nano Lett.* **2003**, *3*, 1049–1051. [[CrossRef](#)]
25. Wang, J.; Tafen, D.N.; Lewis, J.P.; Hong, Z.; Manivannan, A.; Zhi, M.; Li, M.; Wu, N. Origin of Photocatalytic Activity of Nitrogen-Doped TiO<sub>2</sub> Nanobelts. *J. Am. Chem. Soc.* **2009**, *131*, 12290–12297. [[CrossRef](#)]
26. Park, J.H.; Kim, S.; Bard, A.J. Novel Carbon-Doped TiO<sub>2</sub> Nanotube Arrays with High Aspect Ratios for Efficient Solar Water Splitting. *Nano Lett.* **2006**, *6*, 24–28. [[CrossRef](#)]
27. Pinho, L.X.; Azevedo, J.; Miranda, S.M.; Angelo, J.; Mendes, A.; Vilar, V.J.P.; Vasconcelos, V.; Boaventura, R.A.R. Oxidation of microcystin-LR and cylindrospermopsin by heterogeneous photocatalysis using a tubular photoreactor packed with different TiO<sub>2</sub> coated supports. *Chem. Eng. J.* **2015**, *266*, 100–111. [[CrossRef](#)]
28. Lv, H.; Li, N.; Zhang, H.; Tian, Y.; Zhang, H.; Zhang, X.; Qu, H.; Liu, C.; Jia, C.; Zhao, J.; et al. Transferable TiO<sub>2</sub> nanotubes membranes formed via anodization and their application in transparent electrochromism. *Sol. Energy Math. Sol. C* **2016**, *150*, 57–64. [[CrossRef](#)]
29. Su, Z.; Zhou, W. Formation mechanism of porous anodic aluminium and titanium oxides. *Adv. Mater.* **2008**, *20*, 3663–3667. [[CrossRef](#)]
30. Grilli, R.; di Camillo, D.; Lozzi, L.; Horovitz, I.; Mamane, H.; Avisar, D.; Baker, M. Surface characterisation and photocatalytic performance of N-doped TiO<sub>2</sub> thin films deposited onto 200 nm pore size alumina membranes by sol-gel methods. *Mater. Chem. Phys.* **2015**, *159*, 25–37. [[CrossRef](#)]
31. Kobayakawa, K.; Murakami, Y.; Sato, Y. Visible-light active N-doped TiO<sub>2</sub> prepared by heating of titanium hydroxide and urea. *J. Photochem. Photobiol. A Chem.* **2005**, *170*, 177–179. [[CrossRef](#)]
32. Matsushita, M.; Nosaka, A.Y.; Nishino, J.; Nosaka, Y. Preparation of Nitrogen Doped Titanium Dioxide by Using Guanidine and Its Characterization. In *Journal of the Ceramic Society of Japan, Supplement Journal of the Ceramic Society of Japan*; The Ceramic Society of Japan: Gifu, Japan, 2004; pp. S1411–S1413.
33. Senthilnathan, J.; Philip, L. Photocatalytic degradation of lindane under UV and visible light using N-doped TiO<sub>2</sub>. *Chem. Eng. J.* **2010**, *161*, 83–92. [[CrossRef](#)]
34. Wang, X.; Meng, S.; Zhang, X.; Wang, H.; Zhong, W.; Du, Q. Multi-type carbon doping of TiO<sub>2</sub> photocatalyst. *Chem. Phys. Lett.* **2007**, *444*, 292–296. [[CrossRef](#)]